Trans. Phenom. Nano Micro Scales, 1(2): 75-92, Summer – Autumn 2013
DOI: 10.7508/tpnms.2013.02.001

ORIGINAL RESEARCH PAPER

Mixed Convection of Variable Properties Al_2O_3-EG-Water Nanofluid in a Two-Dimensional Lid-Driven Enclosure

G.A. Sheikhzadeh[*,1] , H. Khorasanizadeh[1], S.P. Ghaffari[1]
[1]Department of Thermofluids, Faculty of Mechanical Engineering and Energy Research Institute, University of Kashan, Kashan, Iran

Abstract

In this paper, mixed convection of Al_2O_3-EG-Water nanofluid in a square lid-driven enclosure is investigated numerically. The focus of this study is on the effects of variable thermophysical properties of the nanofluid on the heat transfer characteristics. The top moving and the bottom stationary horizontal walls are insulated, while the vertical walls are kept at different constant temperatures. The study is carried out for Richardson numbers of 0.01–1000, the solid volume fractions of 0–0.05 and the Grashof number of 10^4. The transport equations are solved numerically with a finite volume approach using the SIMPLER algorithm. The results show that the Nusselt number is mainly affected by the viscosity, density and conductivity variations. For low Richardson numbers, although viscosity increases by increasing the nanoparticles volume fraction, due to high intensity convection of enhanced conductivity nanofluid, the average Nusselt number increases for both constant and variable cases. However, for high Richardson numbers, as the volume fraction of nanoparticles increases heat transfer enhancement occurs for the constant properties cases but deterioration in heat transfer occurs for the variable properties cases. The distinction is due to underestimation of viscosity of the nanofluid by the constant viscosity model in the constant properties cases and states important effects of temperature dependency of thermophysical properties, in particular the viscosity distribution in the domain.

Keywords: *Ethylene glycol; Mixed convection; Nanofluid; Variable properties*

1. Introduction

Mixed convection heat transfer is perhaps one of the most frequently encountered physical processes in applied engineering, such as in solar collectors, cooling of electronic devices, heat exchangers, materials processing, metal coating and casting. Numerous studies on lid-driven cavity flow and heat transfer involving different cavity configurations for pure fluid have been published in the literature.

For example, Sharif [1] investigated laminar mixed convection in shallow inclined rectangular cavity with aspect ratio of 10, whereas hot moving lid was on the top and the bottom wall was cooled. He concluded that the average Nusselt number increases mildly with cavity inclination angle for forced convection-dominated regime (Ri=0.1) while it increases much more rapidly for natural convection-dominated regime (Ri=10). Khanafer et al. [2] reported a numerical simulation of unsteady mixed convection in a driven cavity using an externally excited sliding lid. Aminossadati and Ghasemi [3] numerically studied mixed convection heat transfer in two- dimensional

[*]Corresponding author
Email Address: sheikhz@kashanu.ac.ir

Nomenclature

c_p	Specific heat at constant pressure (J kg^{-1} K^{-1})
d	Diameter (m)
g	Gravitational acceleration (m s^{-2})
h	Heat transfer coefficient (W m^{-2} K^{-1})
H	The height of the cavity (m)
K	Thermal conductivity (W m^{-1} K^{-1})
L	The length of the cavity (m)
Nu	Local Nusselt number
Nu_{avg}	Average Nusselt number
P	Pressure (Pa)
Pr	Prandtl number
Ri	Richardson number
Re	Reynolds number
Ra	Rayleigh number
Gr	Grashof number
T	Temperature (K)
T_o	Reference temperature, 298 K
u, v	Dimensional x and y components of velocity (m s^{-1})
U_o	Velocity of the moving lid (m s^{-1})
x, y	Dimensional coordinates (m)
X, Y	Dimensionless coordinates

Greek symbols

α	Thermal diffusivity (m^2 s^{-1})
β	Thermal expansion coefficient (K^{-1})
θ	Dimensionless temperature
κ	Boltzmann constant, 1.3806503×10^{-23}, (J K^{-1})
μ	Viscosity (Pa s)
ξ	Ethylene-Glycol volumetric concentration
ρ	Density (kg m^{-3})
ϕ	Particle volumetric concentration
ψ	Stream function
Ω	Ttilt angle

Subscripts

Avg	Average over the cavity length
C	Cold
EG	Ethylene-Glycol
f	Base or pure fluid

Superscripts

*	Dimensionless properties

horizontal channel whit three different heating modes which related to the location of heat source on the left, bottom or right wall of the cavity. As the cavity aspect ratio increased, at a fixed value of Richardson number, noticeable improvement in the heat transfer observed for the three different heating modes considered. Venkatasubbaiah [4] studied the effect of buoyancy on the stability in mixed convection flow over a horizontal plate. The non-similar mixed convection boundary layer equations were solved directly by direct integration method without any approximation for non-similar terms.
Their results showed that the flow becomes less stable as the buoyancy force increases for assisting mixed convection flow and more stable as the buoyancy force increases for the opposing mixed convection flow.

The heat transfer fluids such as water, ethylene glycol or propylene glycol are used in many industrial applications. Low thermal conductivity is a primary limitation in the development of energy-efficient heat transfer fluids. Therefore, a new class of heat transfer fluids, called nanofluids, can be designed by suspending metallic nanoparticles in conventional heat transfer fluids. During near the two last decades, nanofluids have attracted more attention of the heat transfer community. Use of metallic nanoparticles with high thermal conductivity will increase the effective thermal conductivity of these types of fluids remarkably. Experimental and numerical results show that in forced convection and for a given Reynolds number, the convective heat transfer coefficient increases by increasing the particles volume fraction [5-8]. However, enhancement of natural convection heat transfer by using nanofluids is still controversial; thus, there is a debate on the role of nanoparticles on heat transfer enhancement in natural convection applications.

During the last couple of years, numerous studies on lid-driven cavity flow and heat transfer for nanofluids have been done. Tiwari and Das [9] numerically investigated the behavior of copper–water nanofluid in a two sided lid-driven differentially heated cavity. They considered

different cases characterized by the direction of movement of walls and found that both the Richardson number and the direction of moving walls influence the fluid flow and thermal behavior. Muthtamilselvan et al.[10] numerically studied the mixed convection in a lid-driven enclosure filled with copper–water nanofluid for various aspect ratios. It was shown that both the aspect ratio and solid volume fraction affect the fluid flow and heat transfer in the enclosure. Talebi et al. [11] numerically investigated the flow pattern and temperature fields in a lid-driven cavity utilizing copper–water nanofluid. They showed at a given Reynolds and Rayleigh numbers, solid concentration has a positive effect on heat transfer enhancement. A numerical investigation of mixed convection flow through a copper–water nanofluid in a square cavity with inlet and outlet ports was executed by Shahi et al. [12]. They investigated the effect of presence of. nanoparticles on the hydrodynamic and thermal characteristics of flow at various Richardson numbers. Abu-nada and Chamkha [13] numerically investigated the effect of nanoparticles volume fraction and enclosure inclination angle on the heat transfer characteristics for steady mixed convection flow in a lid-driven inclined square enclosure filled with water-Al2O3 nanofluid. They found that the heat transfer mechanisms and the flow characteristics inside the cavity are strongly dependent on the Richardson number. Also addition of nanoparticles to the base fluid in mixed convection causes enhancement in heat transfer, which is accentuated by inclination of the enclosure. Billah et al. [14] made a numerical investigation of copper-water nanofluid heat transfer in an inclined lid-driven triangular enclosure by using the Galerkin finite element method. Numerical results were obtained for a wide range of parameters such as the Richardson number, tilt angle and nanofluid volume fraction. It was found that the tilt angle strongly affects the fluid flow and heat transfer in the enclosure at the three convective regimes. Chamkha and Abu-nada [15] investigated the steady laminar mixed convection flow and heat transfer of a nanofluid made up of water and Al_2O_3 in single and double lid-driven square cavities. They considered the effect of viscosity models, hence used two models to approximate nanofluid viscosity. They found that increase in volume fraction of nanoparticles causes heat transfer enhancement at moderate and large Richardson numbers using both nanofluid models for both single and double lid cavity configuration. However, for small Richardson number one of the models predicted reduction in the average Nusselt number with increasing in volume fraction of nanoparticles. Khorasanizadeh et al. [16] studied the effect of Reynolds number, Rayleigh number and use of Cu-water nanofluid on thermal and flow characteristics and entropy generation in a lid-driven square cavity. They showed that use of nanofluid causes a higher intensity flow and thus induces the heat transfer and produces a higher Nusselt number. Sheikhzadeh et al. [17] numerically investigated the steady laminar mixed convection flow in a concentric annulus with rotating inner cylinder filled with Al2O3-water nanofluid. They found that the average Nusselt number decreases with increasing the Reynolds number and increases by increasing the Rayleigh number.

Up to now, most numerical studies have used the Brinkman model for viscosity [18] and Maxwell model for thermal conductivity [19]. These models have some defects. The Brinkman model does not consider the effect of nanofluid temperature and nanoparticles size. The Maxwell model is regardless of temperature and the Brownian motion, which is an important mechanism for heat transfer in nanofluids. Namburu et al. [20] studied experimentally the effect of nanoparticles concentration and nanoparticles size on nanofluids viscosity under a wide range of temperatures. The nanofluid used in their experiments was a mixture of 60:40 (by mass) Ethylene-Glycol and water (EG-water) containing CuO nanoparticles. They inferred that for different volume fraction of nanoparticles the nanofluid viscosity drops with temperature. Also in another study, Namburu etal. [21]investigated experimentally the viscosity and specific heat of nanofluids comprised of silicon dioxide (SiO_2) nanoparticles with various diameters suspended in a 60:40 (by mass) EG-water mixture under a wide range of temperatures. Moreover, Sahoo et al. [22] and Vajjha et al. [23-25] examined experimentally the effect of nanoparticles type on nanofluids thermophysical properties under a wide range of temperatures. The nanofluids used in their experiments were 60:40 (by mass) mixtures of EG-water containing Al_2O_3, Sb_2O_5, SnO_2, ZnO, CuO and SiO_2 nanoparticles. They compared the measured values with predictions of the existing equations for the nanofluid properties. In some cases agreement with the experimental data was not observed. Therefore, from physical point of

view it is evident that the dependence of nanofluid properties on temperature is very important and must be taken into account. Abu-Nada and Chamkha [26] studied the natural convection heat transfer characteristics in a differentially-heated enclosure filled with CuO-EG-water nanofluid using different variable thermal conductivity and viscosity models. Their results showed different behaviors (enhancement or deterioration) in the average Nusselt number as the volume fraction of nanoparticles increased, depending on the combination of CuO-EG-water thermal conductivity and viscosity models employed. In another study Abu-Nada et al. [27] investigated the role of nanofluid variable properties in natural convection in differentially heated enclosures and found that properties variations have major effects on the heat transfer rate. Also, they found that at high Rayleigh numbers the Nusselt number was deteriorated due to increased volume fraction of nanoparticles, but for low Rayleigh number an enhancement in heat transfer was registered.

The only studies presented in the literature for mixed convection of variable properties nanofluid are those of Sheikhzadeh et al. [28] and Mazrouei Sebdani et al. [29]. Sheikhzadeh et al. [28] numerically investigated the laminar mixed convection flow in a lid-driven square enclosure filled with Al_2O_3-water nanofluid with temperature and nanoparticles concentration dependent conductivity and viscosity. They used various models for thermal conductivity and viscosity and for a constant solid volume fraction obtained different values for average Nusselt number. Also at low Richardson numbers, the average Nusselt number was more sensitive to the viscosity and thermal conductivity models. The geometry of Mazrouei Sebdani et al. [29] was double cold sides downward driven square cavity with a constant temperature heat source on the bottom wall and an insulated top wall. They conducted a numerical investigation for Al_2O_3-water nanofluid with temperature and nano- particles concentration dependent thermal conductivity and effective viscosity. They used the experimentally based correlation derived by Abu-Nada et al. [27] for nanofluids viscosity and Chon et al. [30] correlation for conductivity. They reported that when the temperature independent models for the viscosity and the conductivity were used heat transfer increased with increase in nanoparticles volume fraction, for all of Reynolds numbers, Rayleigh numbers and locations of the heater. However, when the Abu-Nada et al. [27] and Chon et al. [30] correlations for the viscosity and the conductivity, respectively, were used, with increase in nanoparticles volume fraction the heat transfer either enhanced or mitigated with respect to that of the base fluid, depending on the Reynolds and Rayleigh numbers.

The objective of this numerical work is to study the effects of variable properties Al_2O_3-EG-water nanofluid on the mixed convection characteristics in a lid-driven square enclosure. Unlike [28, 29], all of the thermophysical properties of the nanofluid are considered temperature dependent and the corresponding correlations are all based on experimental results presented in [22-25]. Other than use of EG-water, as the base fluid instead of water used in [28, 29], the base fluid properties themselves are considered temperature dependent. The heat transfer characteristics are evaluated for the Richardson numbers of 0.01–1000 and volume fractions of nanoparticles of 0.0–0.05, whereas Grashof number is kept constant equal to 10^4. To study the significance of properties variations, the results are compared with the cases in which constant properties are used.

2. Problem Description

Conditions

A schematic view of the cavity considered in the present study is shown in Fig. 1. The length and the height of the cavity are denoted by L and H (L = H), respectively.

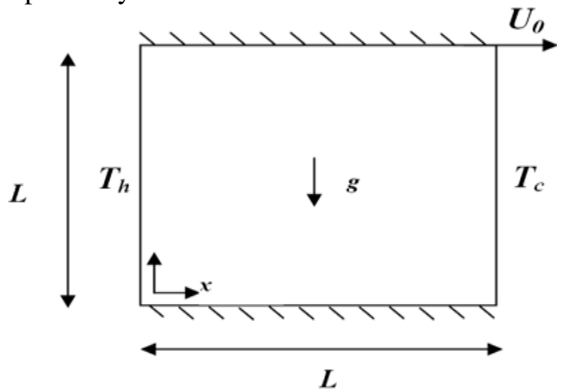

Fig. 1. A schematic diagram of the physical model.

The length of the cavity is considered to be 25 mm. The right wall of the cavity is kept at a constant temperature (T_C) lower than the left hot wall temperature (T_H). The top and bottom horizontal walls are insulated and the top wall is moving with a constant speed (U_0) from left to right. This speed corresponds to the nominated Richardson number.
The boundary conditions are:

$$u = v = 0 \ , \ \partial T / \partial y = 0 \ \text{ at } \ 0 \le x \le L \ \text{ and } \ y = 0 \tag{1a}$$

$$u = U_0 \ , \ v = 0 \ , \ \partial T / \partial y = 0 \ \text{ at } \ 0 \le x \le L \ \text{ and } \ y = H \tag{1b}$$

$$u = v = 0 \ , \ T = T_H \ \text{ at } \ x = 0 \ \text{ and } \ 0 \le y \le H \tag{1c}$$

$$u = v = 0 \ , \ T = T_C \ \text{ at } \ x = L \ \text{ and } \ 0 \le y \le H \tag{1d}$$

The nanofluid in the enclosure is a mixture of 60:40 (by weight) EG-water containing Al_2O_3 nanoparticles. The nanofluid is assumed incompressible and the flow is considered two-dimensional and laminar. According to [22] the nanofluid exhibits a non-Newtonian behavior at a low temperature range of 238 to 273 K for all volume fractions of nanoparticles, such that it behaves as a Bingham plastic with small yield stress that decreases with decreasing volume fraction of nanoparticles and increases with increasing temperature. However, in the temperature range of 273 to 363 K the nanofluid behaves as a Newtonian fluid. In this study, the simulations are performed in the temperature range of 298 to 314.5 K; so the nanofluid is considered Newtonian. In addition, it is assumed that both the EG-water mixture and nanoparticles are in the thermal equilibrium state and flow with the same velocity. The nanoparticles are assumed to have uniform shape and size.

3. Mathematical formulation

The density variation in the body force term of the momentum equation is satisfied by Boussinesq's approximation. The density, viscosity, thermal expansion coefficient, thermal conductivity and the specific heat at constant pressure of the nanofluid are considered variable; all of them change with volume fraction and temperature of nanoparticles. Under the above assumptions, the governing equations are:
Continuity:

$$\frac{\partial}{\partial x}(\rho_{nf} u) + \frac{\partial}{\partial y}(\rho_{nf} v) = 0 \tag{2}$$

x-momentum equation:

$$\frac{\partial}{\partial x}(\rho_{nf} uu) + \frac{\partial}{\partial y}(\rho_{nf} vu) = -\frac{\partial p}{\partial x} + \frac{\partial}{\partial x}\left(\mu_{nf} \frac{\partial u}{\partial x}\right) + \frac{\partial}{\partial y}(\mu_{nf} \frac{\partial u}{\partial y}) \tag{3}$$

$$\frac{\partial}{\partial x}(\rho_{nf} uu) + \frac{\partial}{\partial y}(\rho_{nf} vu) = -\frac{\partial p}{\partial x} + \frac{\partial}{\partial x}\left(\mu_{nf} \frac{\partial u}{\partial x}\right) + \frac{\partial}{\partial y}\left(\mu_{nf} \frac{\partial u}{\partial y}\right)$$

y-momentum equation:

$$\frac{\partial}{\partial x}(\rho_{nf} uv) + \frac{\partial}{\partial y}(\rho_{nf} vv) = -\frac{\partial p}{\partial y} + \frac{\partial}{\partial x}\left(\mu_{nf} \frac{\partial v}{\partial x}\right) + \frac{\partial}{\partial y}\left(\mu_{nf} \frac{\partial v}{\partial y}\right) + g(T - T_C)(\rho\beta)_{nf} \tag{4}$$

Energy equation:

$$\frac{\partial}{\partial x}(\rho_{nf} uT) + \frac{\partial}{\partial y}(\rho_{nf} vT) = \frac{\partial}{\partial x}\left(\frac{k_{nf}}{c_{p_{nf}}} \frac{\partial u}{\partial x}\right) + \frac{\partial}{\partial y}\left(\frac{k_{nf}}{c_{p_{nf}}} \frac{\partial v}{\partial y}\right) \tag{5}$$

Eqs. (2)–(5) are converted to the dimensionless forms by definition of the following parameters:

$$X = x/L \, , Y = y/L \, , U = u/U_0 \, ,$$

$$V = v/U_0 \, , \theta = \frac{T - T_C}{T_H - T_C} \, ,$$

$$P = \frac{p}{\rho_{f,0}(U_0)^2} \, , \quad \rho^* = \frac{\rho_{nf}}{\rho_{f,0}} \tag{6}$$

$$\mu^* = \frac{\mu_{nf}}{\mu_{f,0}} \, , \ k^* = \frac{k_{nf}}{k_{f,0}} \, ,$$

$$c_P^* = \frac{c_{P_{nf}}}{c_{P_{f,0}}}$$

The dimensionless forms of the governing equations are:

$$\frac{\partial}{\partial X}(\rho^* U) + \frac{\partial}{\partial Y}(\rho^* V) = 0 \tag{7}$$

$$\frac{\partial}{\partial X}\left(\rho^* UU\right) + \frac{\partial}{\partial Y}\left(\rho^* VU\right) = -\frac{\partial P}{\partial X} + \frac{1}{Re_{f,0}}\left[\frac{\partial}{\partial X}\left(\mu^* \frac{\partial U}{\partial X}\right) + \frac{\partial}{\partial Y}\left(\mu^* \frac{\partial U}{\partial Y}\right)\right] \tag{8}$$

$$\frac{\partial}{\partial X}\left(\rho^* UV\right) + \frac{\partial}{\partial Y}\left(\rho^* VV\right) = -\frac{\partial P}{\partial Y} + \frac{1}{Re_{f,0}}\left[\frac{\partial}{\partial X}\left(\mu^* \frac{\partial V}{\partial X}\right) + \frac{\partial}{\partial Y}\left(\mu^* \frac{\partial V}{\partial Y}\right)\right] + Ri_{f,0}\rho^* \beta^* \theta \tag{9}$$

$$\frac{\partial}{\partial X}\left(\rho^* U\theta\right) + \frac{\partial}{\partial Y}\left(\rho^* V\theta\right) = \frac{1}{Re_{f,0} Pr_{f,0}}\left[\frac{\partial}{\partial X}\left(\frac{k^*}{c^*}\frac{\partial U}{\partial X}\right) + \frac{\partial}{\partial Y}\left(\frac{k^*}{c^*}\frac{\partial V}{\partial Y}\right)\right] \tag{10}$$

where the Reynolds, Richardson, Grashof and Prandtl numbers, respectively, are:

$$Re_{f,0} = \frac{\rho_{f,0} U_0 L}{\mu_{f,0}},\quad Ri_{f,0} = \frac{Gr_{f,0}}{Re_{f,0}^2},\quad Gr_{f,0} = \frac{g\beta_{f,0}(T_H - T_C)L^3}{\upsilon_{f,0}^2},\quad Pr_{f,0} = \frac{\upsilon_{f,0}}{\alpha_{f,0}} \tag{11}$$

The boundary conditions in the dimensionless form are:

$$U = V = 0,\ \partial\theta/\partial X = 0 \text{ at } 0 \le X \le 1 \text{ and } Y = 0 \tag{12a}$$

$$U = 1, V = 0,\ \partial\theta/\partial X = 0 \text{ at } 0 \le X \le 1 \text{ and } Y = 1 \tag{12b}$$

$$U = V = 0,\ \theta = 1 \text{ at } X = 0 \text{ and } 0 \le Y \le 1 \tag{12c}$$

$$U = V = 0,\ \theta = 0 \text{ at } X = 1 \text{ and } 0 \le Y \le 1 \tag{12d}$$

The heat transfer coefficient on any y at the hot wall is:

$$h = \frac{-k_{nf}\left.\frac{\partial T}{\partial x}\right|_{x=0}}{(T_H - T_C)} \tag{13}$$

and the local Nusselt number is:

$$Nu = \frac{hL}{k_f} \tag{14}$$

Substituting Eq. (13) into Eq. (14) and using the dimensionless quantities, the local Nusselt number along the left wall becomes:

$$Nu = -\left(\frac{k_{nf}}{k_{f,0}}\right)\left.\frac{\partial\theta}{\partial X}\right|_{X=0} \tag{15}$$

where k_{nf} is calculated using Eq. (22) in the constant properties cases and is calculated using Eq. (25) in variable properties cases. Finally, the average Nusselt number is determined from:

$$Nu_{avg} = \int_0^1 Nu dY \tag{16}$$

4.Thermophysical properties of nanofluids

The aim of this work is examination of heat transfer characteristics of the Al_2O_3-EG-water nanofluid using models for variable properties with temperature. However, to show the importance of properties variations the results are compared with those of constant properties models. In this section both variable and constant properties models used in this study are introduced.

4.1. Constant properties models

The effective density of nanofluids, validated experimentally for Al_2O_3-water nanofluid by Pak and Cho [31], is given by:

$$\rho_{nf} = \phi\rho_P + (1-\phi)\rho_f \tag{17}$$

The specific heat and thermal expansion coefficient of nanofluids proposed by [31], respectively, are given by:

$$\left(\rho c_p\right)_{nf} = \phi\left(\rho c_p\right)_P + \left(1-\phi\right)\left(\rho c_p\right)_f \quad (18)$$

$$\left(\rho\beta\right)_{nf} = \phi\left(\rho\beta\right)_P + \left(1-\phi\right)\left(\rho\beta\right)_f \quad (19)$$

The nanofluid viscosity is estimated by the correlation developed by Brinkman [18] as:

$$\mu_{nf} = \frac{\mu_f}{\left(1-\phi\right)^{2.5}} \quad (20)$$

For thermal conductivity of nanofluids numerous theoretical studies have been conducted dating back to the classical work of Maxwell. Maxwell's model states that the effective thermal conductivity of a nanofluid depends on the thermal conductivity of both nanoparticles and the base fluid as well as the volume fraction of nanoparticles. Accordingly, the effective thermal conductivity, given by Wang et al. [19], is:

$$k_{nf,Maxwell} = \frac{k_P + 2k_f - 2\phi\left(k_f - k_p\right)}{k_P + 2k_f + \phi\left(k_f - k_p\right)} k_f \quad (21)$$

For the EG-water mixture:

$$\rho_f = \xi\rho_{EG} + \left(1-\xi\right)\rho_w \quad (22a)$$

$$\left(\rho\eta\right)_f = \xi\left(\rho\eta\right)_{EG} + \left(1-\xi\right)\left(\rho\eta\right)_w \quad (22b)$$

where η is the thermal expansion coefficient of the EG-water mixture and ξ is Ethylene Glycol volumetric concentration in the mixture and is equal to 0.578 for 60:40 EG-water by mass mixture [32]. The properties of nanoparticles, Ethylene Glycol and water at reference temperature are presented in Table 1.

Table 1
Properties of the Al_2O_3 nanoparticles, EG and water at reference temperature of 298 K [33].

Properties	Al_2O_3	EG	water
$\rho\ \left(\text{kg.m}^{-3}\right)$	3970	1114.4	997
$c_p\ \left(\text{J.kg}^{-1}\text{.K}^{-1}\right)$	765	2415	4179
$\mu\ \left(\text{Pa.s}\right)$	-	157×10^{-4}	8.95×10^{-4}
$\beta\ \left(\text{K}^{-1}\right)$	0.846	27.61×10^{-5}	22×10^{-5}
$k\ \left(\text{W.m}^{-1}\text{.K}^{-1}\right)$	36	0.252	0.613

4.2. Variable properties models

As described by Vajjha et al. [25], the best correlation for the density of Al_2O_3 nanoparticles dispersed in 60:40 EG-water mixture is presented by Eq. (17). The variable density of EG-water, as the base fluid, proposed by Vajjha et al. [34] is:

$$\rho_f = -2.43\times10^{-3}T^2 + 0.96216T + 1009.9261 \quad (23)$$

The specific heat of Al_2O_3-EG-w nanofluid for 60:40 by mass EG-water mixture given by Vajjha and Das [24] is:

$$\frac{c_{p,nf}}{c_{p,f}} = \frac{8.911\times10^{-4}T + 0.5179\dfrac{c_{p,p}}{c_{p,f}}}{0.425+\phi} \quad (24)$$

Sahoo et al. [22] measured the viscosity of Al_2O_3-EG-water nanofluid for volume fractions of up to 0.1. For the temperature range of 273 to 363 K, they proposed:

$$\mu_{nf} = 2.392\times10^{-7}\exp\left(\frac{2903}{T} + 12.65\phi\right) \quad (25)$$

Vajjha and Das [23] measured the thermal conductivity of Al_2O_3-EG-water nanofluid for60:40 EG-water mixture. They developed a thermal conductivity model as a two-term function in the temperature range of 298 to 363 K as:

$$k_{nf}=\frac{k_P+2k_f-2\phi\left(k_f-k_p\right)}{k_P+2k_f+\phi\left(k_f-k_p\right)}k_f+ 5\times10^4 B\phi\rho_f c_{p,f}\sqrt{\frac{\kappa T}{\rho_p d_p}}f(T,\phi) \quad (26a)$$

where $f(T,\phi)$ is:

$$f(T,\phi)=\left(2.8217\times10^{-2}\phi+3.917\times10^{-3}\right)\frac{T}{T_0}+\left(-3.0669\times10^{-2}\phi-3.91123\times10^{-3}\right) \quad (26b)$$

B is fraction of the liquid volume which travels with a particle and for nanofluid comprised of Al_2O_3 nanoparticles is:

$$B=8.4407(100\phi)^{-1.07304} \quad (26c)$$

The first term in Eq. (26-a) is called the static part and the second term takes into account the effect of particle size, particle volume fraction, temperature and properties of the base fluid as well as the nanoparticles subjected to Brownian motion.

To the best of our knowledge, there is no correlation for thermal expansion coefficient of Al_2O_3-EG-water as a function of temperature; thus in this study Eq. (19) has been used as a base to obtain a variable thermal expansion coefficient. For this purpose, the values of density and thermal expansion coefficient of EG and water taken from [33], within the temperature range of 290-320 K, have been curve fitted firstly. The results are:

$$\rho_{EG}=4.667\times10^{-4}T^3-0.4515T^2+144.1T-1.408\times10^4 \quad (27)$$

$$\beta_{EG}=6.5\times10^{-4} \quad (28)$$

$$\rho_w=-0.003404T^2+1.726T+785.1 \quad (29)$$

$$\beta_w=\left(-0.0610T^2+45.9T-7999\right)\times10^{-6} \quad (30)$$

Then the thermal expansion coefficient of the EG-water mixture has been obtained using Eq. (22-b). Finally, by substituting the results in Eq. (19) the thermal expansion coefficient of nanofluid has been obtained as:

$$(\rho\beta)_f=0.578\times[(4.667\times10^{-4}T^3-0.4515T^2+144.1T-1.408\times10^4)\times(6.5\times10^{-4})]EG+0.422\times[(-0.003404T^2+1.726T+785.1)\times\left((-0.0610T^2+45.9T-7999)\times10^{-6}\right)]_w \quad (31)$$

The other properties of the base fluid are [34]:

$$\mu_f=5.55\times10^{-7}\exp\left(\frac{2664}{T}\right) \quad (32)$$

$$k_f=-3.196\times10^{-6}T^2+2.512\times10^{-3}T-0.10541 \quad (33)$$

$$c_{p,f}=4.2483T+1882.4 \quad (34)$$

5. Numerical method

The governing equations have been solved numerically based on the finite volume method using a collocated grid system. Central difference scheme has been used to discretize the diffusion terms, whereas a hybrid scheme (a combination of the central difference scheme and the upwind scheme) has been employed to approximate the convection terms. The SIMPLER-algorithm has been adopted to solve for the pressure and the velocity components. The coupled set of discretized equations have been solved iteratively using the TDMA method [35]. To obtain converged solution an under-relaxation scheme has been employed.

5.1. Validation of the results

In order to validate the numerical procedure the geometry and conditions of Talebi et al. [11] have been considered for two particular test cases. The test cases are the mixed convection of water as base fluid and Cu-water nanofluid in a two-dimensional square enclosure. Table 2 and Table 3 show the average Nusselt number on the hot wall for base fluid and nanofluid with ϕ=0.05, respectively, for various Reynolds and Rayleigh numbers obtained by the results of the computer code of this study compared with those of Talebi et al. [11]. It should be noted

that the values for average Nusselt numbers have been picked from related curves in [11] with ultimate care. As seen, for base fluid and the nanofluid with ϕ=0.05 good agreement exist between the average Nusselt numbers obtained in this study and those of Talebi et al. [11].

Table 2
Nu_{avg} for the base fluid; comparison with [11] for validation of the numerical results.

Re	*Ra*	Nu_{avg} **(Talebi et al. [11])**	Nu_{avg} **(Present study)**
1	1.47×10^4	3	2.85
10	1.47×10^5	5.9	6.08
100	1.47×10^6	11.9	12.72

Table 3
Nu_{avg} for the nanofluid with ϕ=0.05; comparison with [11] for validation of the numerical results.

Re	*Ra*	Nu_{avg} **(Talebi et al. [11])**	Nu_{avg} **(Present study)**
1	1.47×10^4	3.9	3.98
10	1.47×10^5	7.9	8.21
100	1.47×10^6	17.1	17.05

5.2. Grid independency study

To perform grid independent examination, the numerical procedure has been conducted for one of the test cases of this study with different grid resolutions. Table 4 demonstrates the influence of number of grid points on the average Nusselt number. The relative difference of the average Nusselt number for grid system of 181×181 compared with that of 161×161 is less that 0.3%. Therefore, the grid system of 161×161 has been fine enough to obtain accurate results, thus was adopted in all of the subsequent simulations.

Table 4
Nu_{avg} for $Gr = 10^4$, $Ri_{f,0}$=1 and ϕ=0.05 in the mesh refinement study.

Number of grids	Nu_{avg}
41×41	12.62
61×61	12.24
81×81	11.94
101×101	11.73
121×121	11.58
141×141	11.48
161×161	11.39
181×181	11.36

6. Results and discussion

In this section, a representative set of graphical results are presented to illustrate the influence of the various physical parameters on heat transfer characteristics of the mixture of 60:40 EG-water containing Al_2O_3 nanoparticles in the square lid-driven cavity. For the variable property cases all of the thermophysical properties of the nanofluid and the base fluid have been considered variable. Since the boundary conditions and the thermophysical properties have strong effect on the heat transfer rate, the numerical computations were performed for a range of $Ri_{f,0}$ and ϕ ($Ri_{f,0}$=0.01–1000 and ϕ=0.0–0.05) but the Grashof number was assumed to be constant (Gr=10^4). It should be noted that the Reynolds number varies with variation of the Richardson number. In this study, the right cold wall temperature has been maintained at 298 K, thus for Grashof number of 10^4 and dependent on the properties of the base fluid and the characteristic length of the cavity (25mm) the temperature difference between the hot and cold walls is approximately 16.5 ^{o}C, hence the hot wall temperature is 314.5 K.

In order to emphasis on the importance of variation of properties with temperature the values of different properties at 298 and 314.5 K (on the right and cold walls) for the case with ϕ=0.05 and $Ri_{f,0}$=1 have been presented in Table 5.

As noticed, by increasing the temperature from 298 to 314.5 K the viscosity of nanofluid has decreased almost 38%. Due to dependency of viscosity on temperature and according to the temperature field in the domain there is viscosity distribution across the cavity.

Table 5
The properties of the nanofluid with ϕ=0.05 and $Ri_{f,0}$ =1 at the hot and cold temperatures

Properties	T_c=298 K	T_h=314.5 K
ρ_{nf} $\left(\text{kg.m}^{-3}\right)$	1225.3	1217.6
$c_{p,nf}$ $\left(\text{J.kg}^{-1}.\text{K}^{-1}\right)$	2723.9	2594.1
μ_{nf} (Pa.s)	7.65×10^{-3}	4.74×10^{-3}
β_{nf} $\left(\text{K}^{-1}\right)$	4.52×10^{-4}	4.12×10^{-4}
k_{nf} $\left(\text{W.m}^{1}.\text{K}^{-1}\right)$	0.4310	0.4095

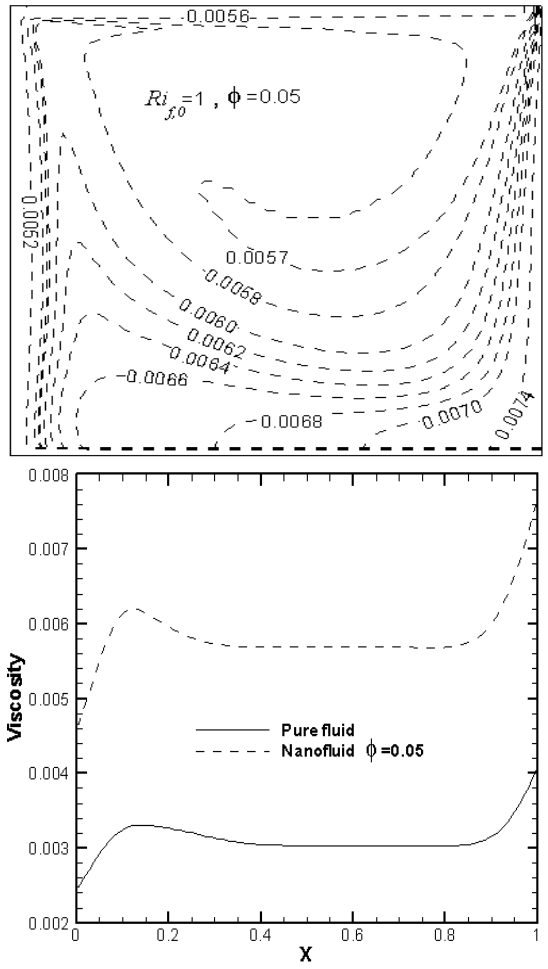

Fig. 2. (a) Contour map of the nanofluid viscosity in the cavity. (b) Viscosity of the nanofluid and the base fluid at the midsection of the cavity, both for $Ri_{f,0}$ =1.

This viscosity distribution is noticed from Fig. 2a for the case with ϕ=0.05 and $Ri_{f,0}$=1. Also from Fig. 2b it is noticed that for the nanofluid with ϕ=0.05 and $Ri_{f,0}$=1 the viscosity of the nanofluid on the midsection line of the cavity (Y=0.5) is more than that of the base fluid for the same $Ri_{f,0}$.

Due to variation of density with temperature, for studying the flow field in the variable cases the term $\rho\psi$, called flow strength, is more important than stream function (ψ). Fig. 3 presents the contour maps of $\rho\psi$ at different $Ri_{f,0}$ for the base fluid and the nanofluid with ϕ=0.05. At $Ri_{f,0}$=0.01 and 0.1, for which the forced convection is dominant a relative vacuum zone occurs at the left top corner (see Figs. 3a-b). By increasing $Ri_{f,0}$, the Reynolds number decreases, hence the effect of lid-driven and forced convection decreases. At $Ri_{f,0}$= 100 and 1000, natural convection is more effective than forced convection and, as can be seen from Fig. 3f, the flow pattern becomes symmetric. The use of nanofluid, even with ϕ=0.05, does not have a major effect on the flow pattern, however augments the flow intensity. The maximum value of the flow strength for the base fluid with $Ri_{f,0}$=0.01 is 115.02 but for the nanofluid with $Ri_{f,0}$=0.01 and ϕ=0.05 is 119.83 showing almost 4% enhancement and the maximum values of flow strength at $Ri_{f,0}$=1000 are 176.25 and 188.8 for the base fluid and nanofluid with ϕ =0.05, respectively, which shows almost 7% enhancement for the nanofluid. The variation of the vertical velocity at the middle of the enclosure for the base fluid and the nanofluid with ϕ=0.05 at different Richardson numbers are shown in Fig. 4. At low $Ri_{f,0}$=0.01 and 0.1, due to the motion of the lid, the forced convection is dominant so the y-velocity distribution along the middle line of the cavity is unsymmetrical. However, by increasing $Ri_{f,0}$ to 100 and then 1000 the natural convection becomes dominant, hence symmetry is observed. As shown in Fig. 4, by using the nanofluid with ϕ=0.05 instead of the base fluid, increased viscosity causes the velocity to attenuate, hence the maximum vertical velocity at mid-plane decreases. In Fig. 5 isotherms are shown for the base fluid and the nanofluid with ϕ=0.05 at different Richardson numbers. At low $Ri_{f,0}$=0.01 and 0.1 a thick thermal boundary layer adjacent to the vertical walls exists and a vast region of the cavity is at the same temperature. By decreasing the lid velocity (increasing $Ri_{f,0}$) the natural convection dominates and temperature distribution extends to the whole cavity.

Fig. 6 shows the variation of the local Nusselt number (*Nu*) along the hot wallfor base fluid and the nanofluid with ϕ =0.03 and 0.05 and Richardson numbers of 0.01, 0.1, 100 and 1000. The variation of local Nusselt number along the hot wall for the base fluid and the nanofluid at low $Ri_{f,0}$ of 0.01 and 0.1 is totally different compared to those of $Ri_{f,0}$=100 and 1000.

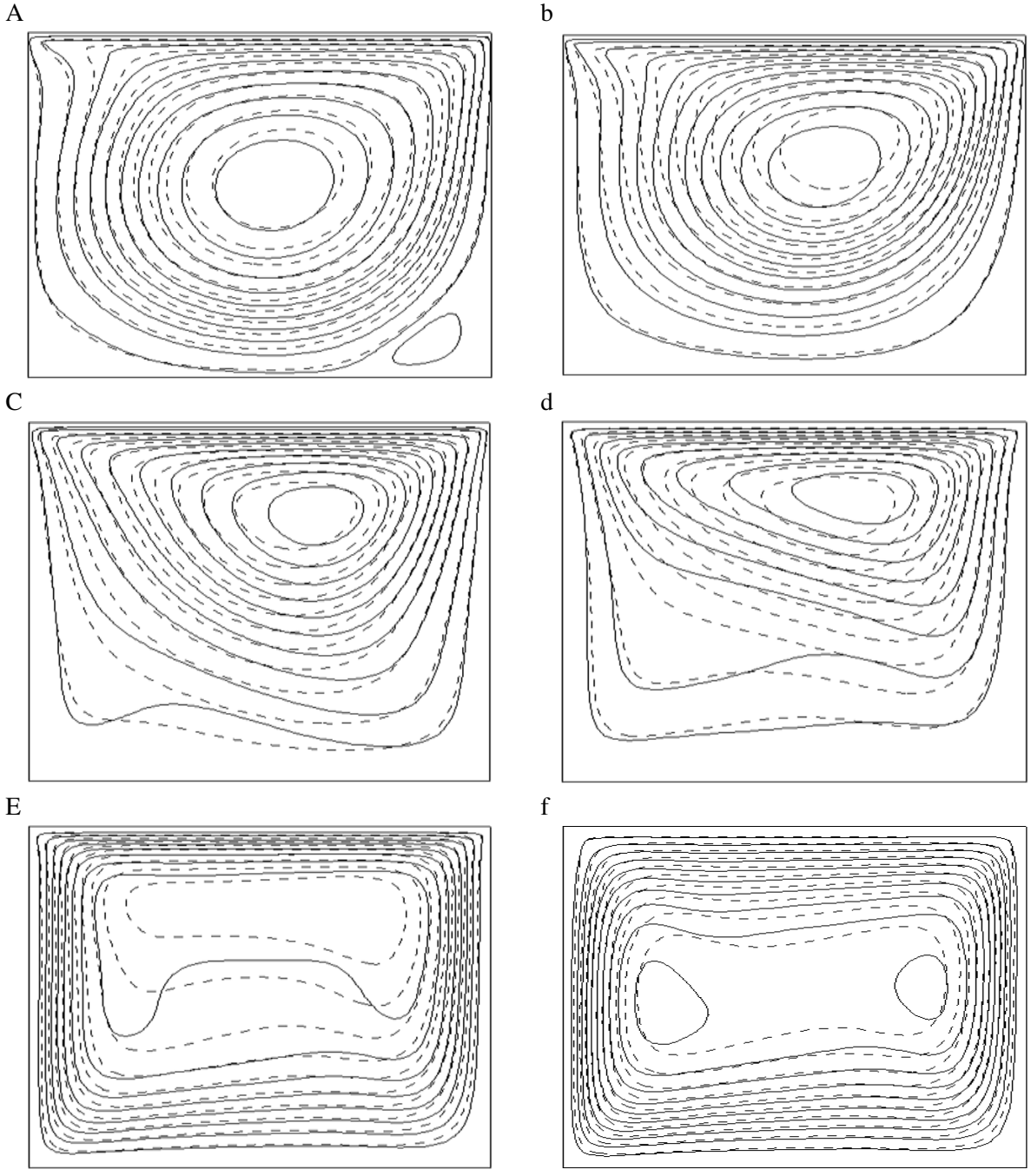

Fig. 3. Flow strength for the nanofluid (ϕ=0.05 dashed lines) and the base fluid (solid lines); a) $Ri_{f,0}$=0.01 b) $Ri_{f,0}$=0.1 c) $Ri_{f,0}$=1 d) $Ri_{f,0}$=10 e) $Ri_{f,0}$=100 f) $Ri_{f,0}$=1000.

At low $Ri_{f,0}$ the forced convection dominance and noticeable temperature difference between the convective media and the hot wall initially causes increase of *Nu* with Y such that it arrives at its first maximum value at almost Y=0.4. Then it decreases first but increases again to its highest value at Y=1. This increase is due to the motion of the lid which causes secondary vortexes at the top left corner of the cavity. However, as $Ri_{f,0}$ increases the effect of moving lid becomes negligible, hence the natural convection becomes dominant and the *Nu* increases for Y<0.1 but decreases at all higher Y values. The differences observed between the variation of *Nu* with Y for the nanofluid and for the base fluid are related to the variation of viscosity and conductivity of nanofluid with temperature and ϕ. For instance at $Ri_{f,0}$=1000, for which natural convection is dominant, due to higher viscosity of the nanofluid compared with the base fluid, the nanofluid *Nu* is lower than that of base fluid everywhere on the hot wall. Temperature gradient along the hot wall for base fluid and nanofluid with ϕ=0.03 and 0.05 and thermal conductivity ratio versus volume fraction of nanoparticles at $Ri_{f,0}$=0.01 and 1000 are shown in Fig. 7. These figures are echo of Fig. 6 and explain the reasons for the kind of variation of *Nu* with Y at different $Ri_{f,0}$ values. According to equation (15), the Nusselt number is influenced by temperature gradient at the left hot wall as well as thermal conductivity ratio.

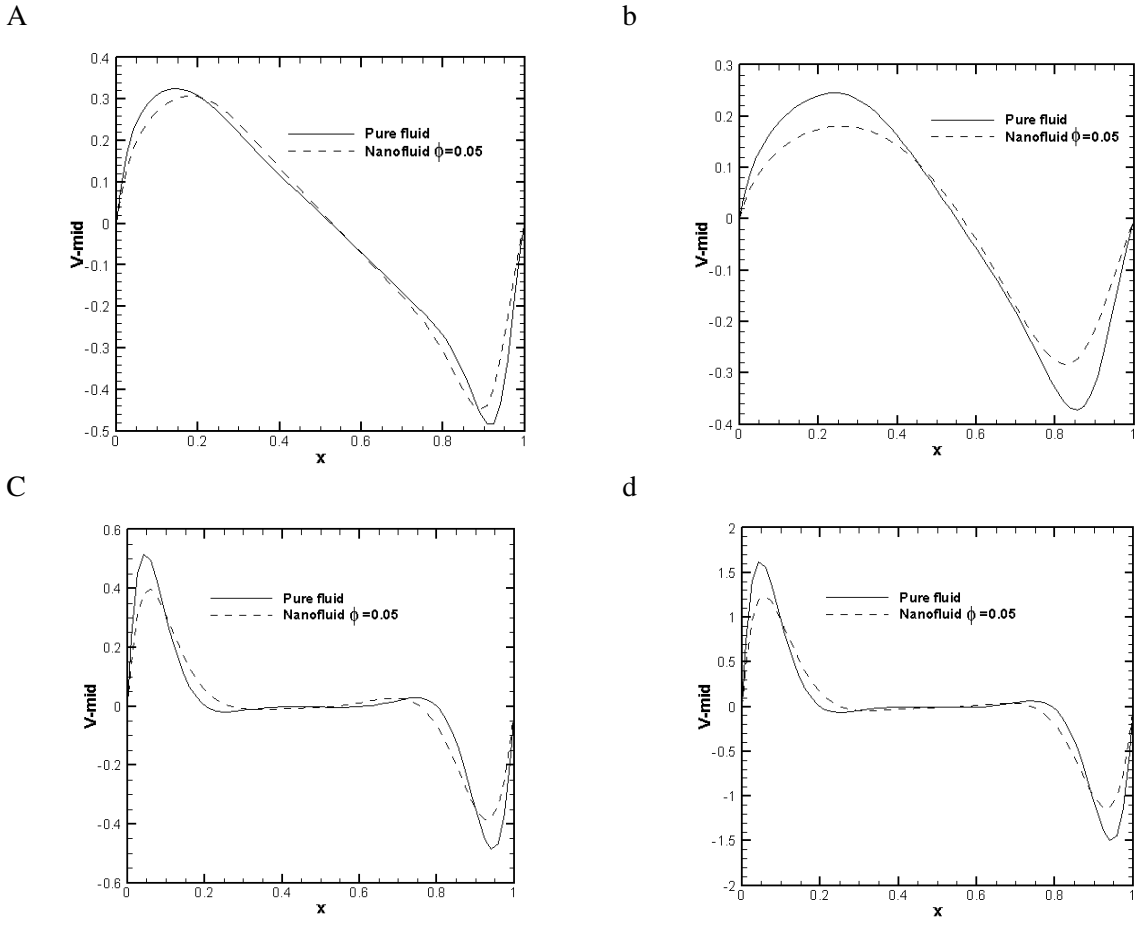

Fig. 4. y-velocity at the midsection of the enclosure (Y=0.5) for the nanofluid with ϕ=0.05 and base fluid; a) $Ri_{f,0}$=0.01 b) $Ri_{f,0}$=0.1 c) $Ri_{f,0}$=100 d) $Ri_{f,0}$=1000.

For instance for $Ri_{f,0}$=1000, the viscosity of the nanofluid increases with increased ϕ and the temperature gradient on the heated wall decreases but the thermal conductivity ratio increases. However, the effect of the temperature gradient decrease is more important, such that for the nanofluid with ϕ=0.05 compared to the base fluid there is 18% increase for thermal conductivity ratio and maximum 28.2% decrease for temperature gradient; thus the maximum *Nu* decreases accordingly. To show the importance of the variation of the properties with temperature the results obtained using variable properties need to be compared with those of constant properties. It should be noted that the properties in the constant property simulations (given by Eqs. 17-22) have been evaluated at the reference temperature of 298 K.

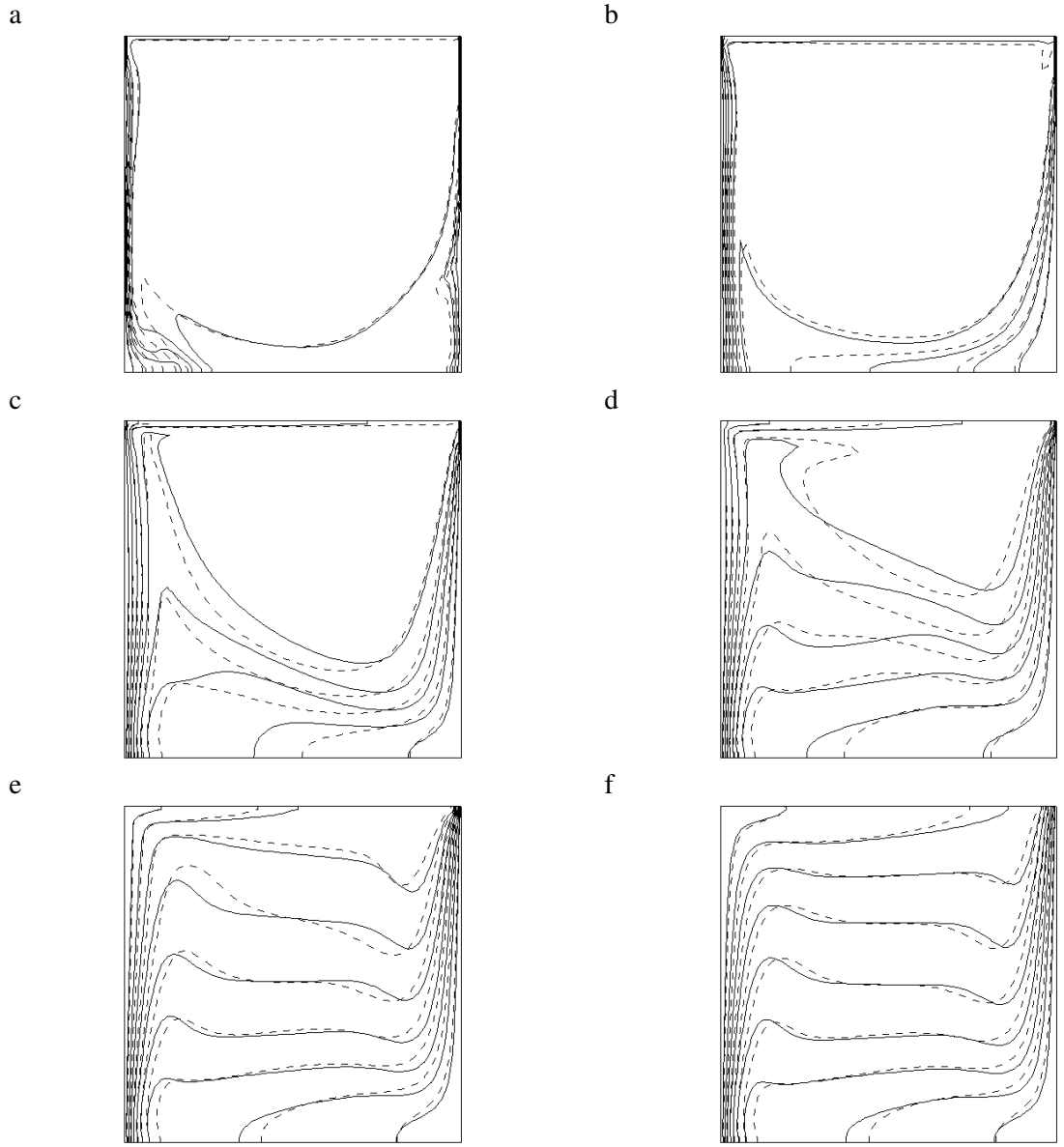

Fig. 5. Isotherms for the nanofluid with ϕ=0.05 and the base fluid. a) $Ri_{f,0}$=0.01 b) $Ri_{f,0}$=0.1 c) $Ri_{f,0}$=1 d) $Ri_{f,0}$=10 e) $Ri_{f,0}$=100 f) $Ri_{f,0}$=1000.

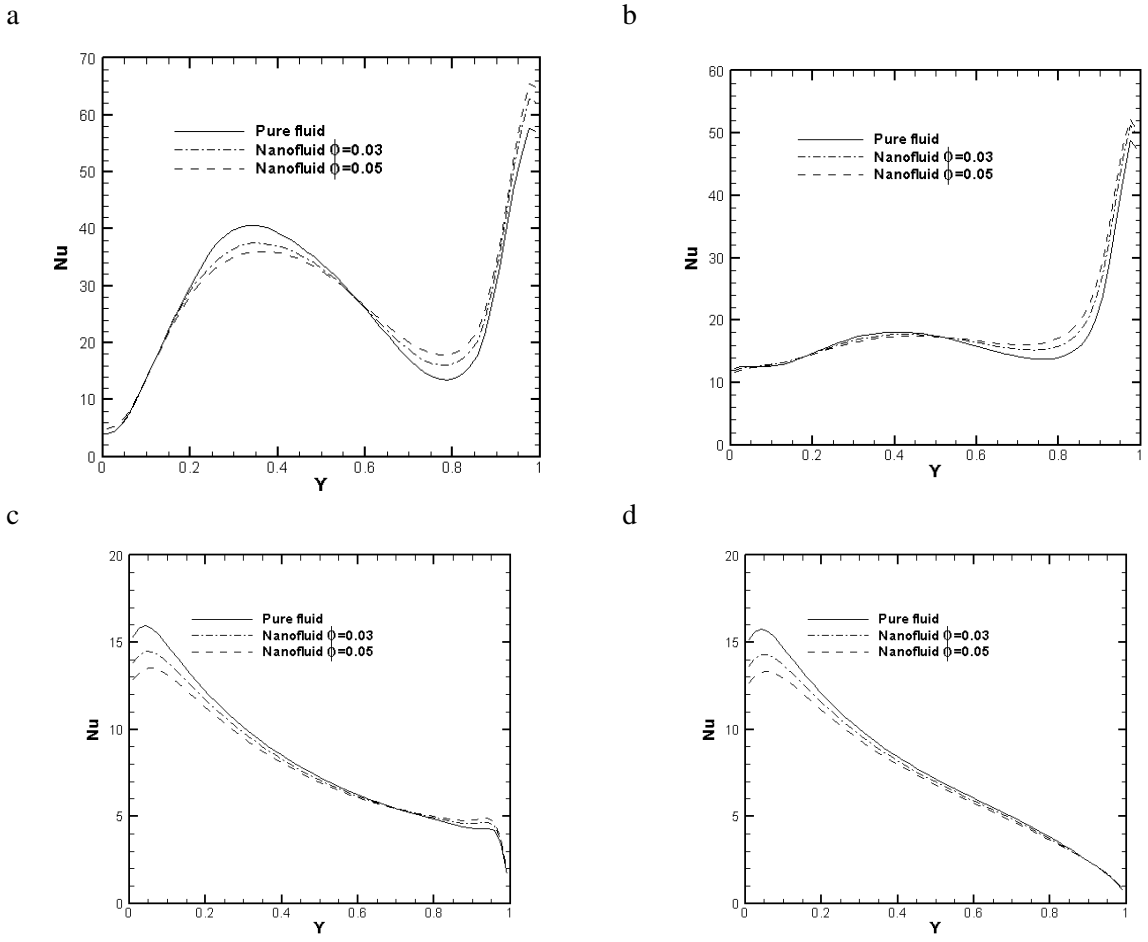

Fig. 6. The local Nusselt number along the hot wall for the base fluid and the nanofluid with ϕ=0.03 and 0.05; a) $Ri_{f,0}$=0.01 b) $Ri_{f,0}$=0.1 c) $Ri_{f,0}$=100 d) $Ri_{f,0}$=1000.

The Nu_{avg} on the hot wall for the constant as well as the variable properties cases are shown in Fig. 8 for Richardson numbers of 0.01–1000. It is seen that at low $Ri_{f,0}$ of 0.01, 0.1 and 1, by increasing the volume fraction of nanoparticles, Nu_{avg} increases in constant and variable properties cases. This is in agreement with the results of Talebi et al. [11] and Abu-nada and Chamkha [13]. However, the rate of Nu_{avg} enhancement is linear also is higher when constant properties have been used. Addition of nanoparticles increases the conductivity, the viscosity and the density of the nanofluid. Thus, the nanofluid with ϕ=0.05 is more conductive, more dense and more viscous compared with the base fluid. At low Richardson values, for which the forced convection is dominant, the higher conductivity of the nanofluid enhances heat transfer, despite its higher viscosity. The differences observed between the Nu_{avg} values in the constant properties cases compared with those of the variable properties cases at any ϕ is related to the fact that in the variable properties cases completely different models have been used for the properties. At high $Ri_{f,0}$ of 10, 100 and 1000, for which the natural convection is dominant, by increasing the volume fraction of nanoparticles the average Nusselt increases for constant properties cases, similar to what was observed by Ghasemi and Aminossadati [36], but decreases for variable properties cases. This distinction is due to underestimation of viscosity of the nanofluid in the constant properties models (see Fig. 2b) and states the important effects of temperature dependency of thermophysical properties, in particular the viscosity distribution in the domain (see Fig 2a). At higher Richardson values, for which the effect of moving lid is very weak, although the addition of nanoparticles increases conductivity of the nanofluid, the higher viscosity of the nanofluid causes heat transfer decrease.

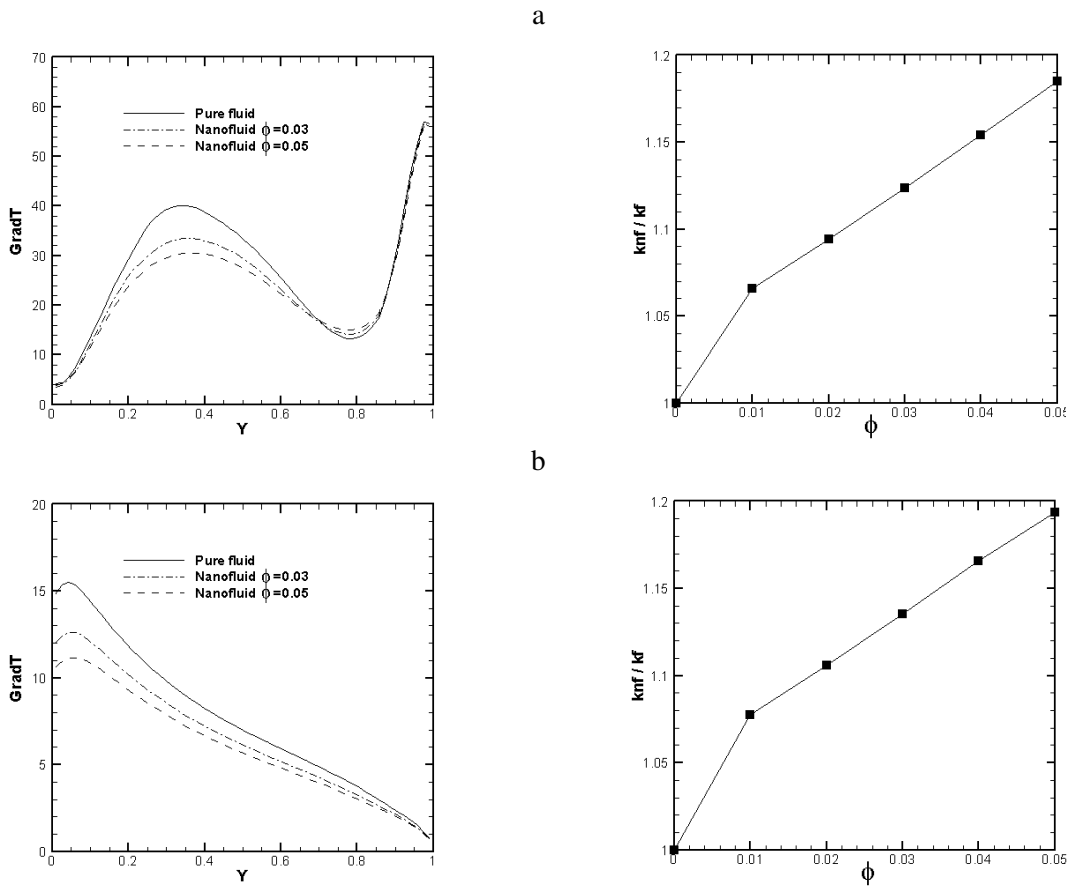

Fig. 7. The temperature gradient along the hot wall for the base fluid and the nanofluid and the thermal conductivity ratio; a) $Ri_{f,0}$=0.01 b) $Ri_{f,0}$=1000.

7. Conclusions

The mixed convection of variable properties Al_2O_3-EG-water nanofluid in a lid-driven enclosure was studied numerically. For constant Grashof number of 10^4, various nanoparticles volume fractions and Richardson numbers were considered and the flow and temperature fields as well as heat transfer characteristics were studied. To study the effects of temperature dependent thermophysical properties the heat transfer results for the variable properties cases were compared with those of constant properties cases. It was shown that the changes of the properties influence the flow field as well as the heat transfer characteristics. The Nusselt number is mainly affected by the viscosity and density but the heat transfer predictions are insensitive to the thermal conductivity ratio. For low Richardson numbers ($Ri_{f,0}$=0.01, 0.1 and 1) due to driven lid the forced convection is dominant, thus although viscosity increases by increasing the nanoparticles volume fraction the average Nusselt number increases due to high intensity convection of enhanced conductivity nanofluid. However, for high Richardson numbers ($Ri_{f,0}$=10, 100 and 1000) and as the volume fraction of nanoparticles increased the results showed heat transfer enhancement for the constant properties cases but deterioration in heat transfer for the variable properties cases. This distinction is due to underestimation of viscosity of the nanofluid in the constant properties models and states the important effects of temperature dependency of thermophysical properties, in particular the viscosity distribution in the domain.

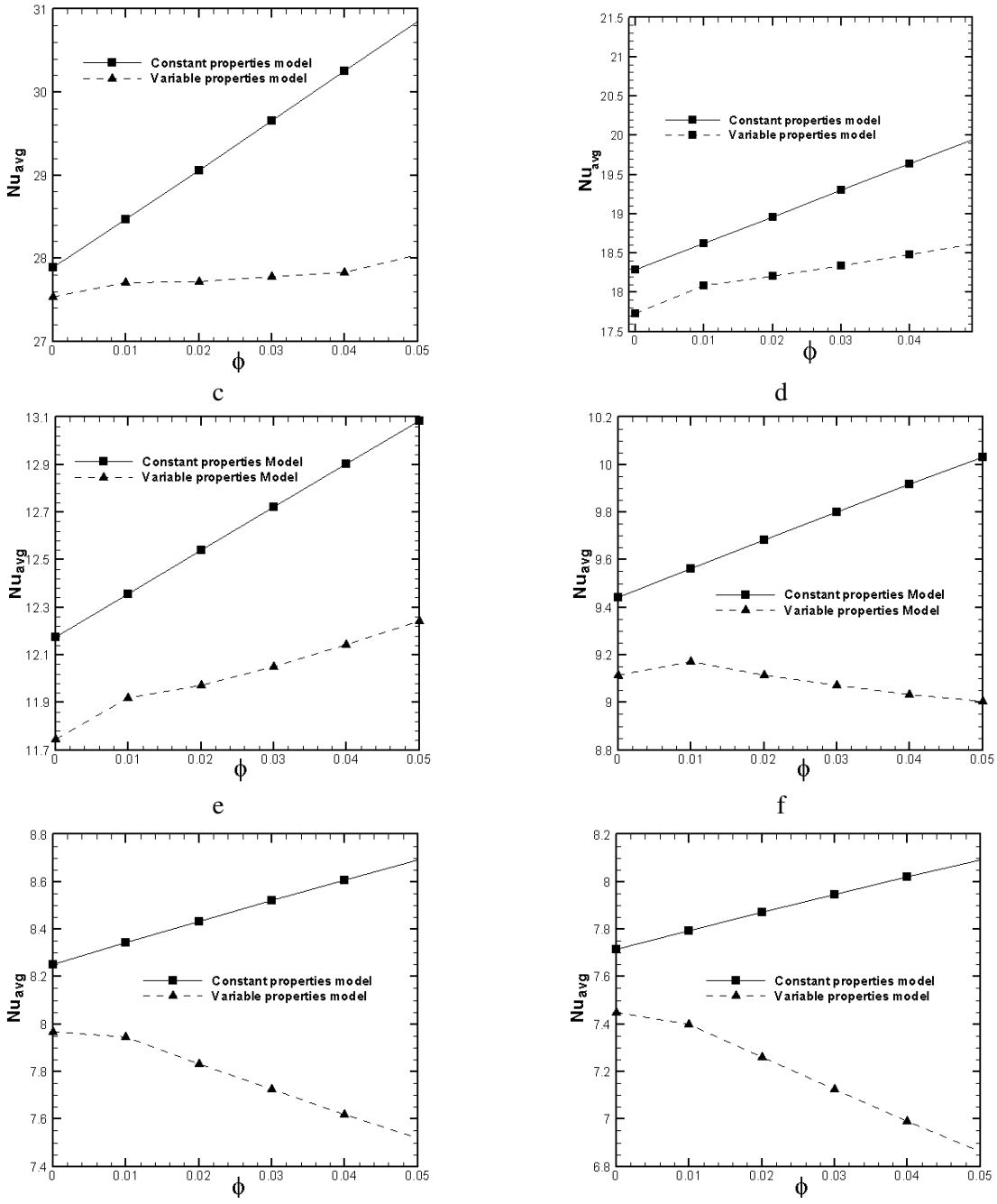

Fig. 8. The average Nusselt number for a) $Ri_{f,0}$=0.01 b) $Ri_{f,0}$=0.1 c) $Ri_{f,0}$=1 d) $Ri_{f,0}$=10 e) $Ri_{f,0}$=100 f) $Ri_{f,0}$=1000; comparison between the constant and the variable properties cases.

References

[1] M.A.R. Sharif, Laminar mixed convection in shallow inclined driven cavities with hot moving lid on top and cooled from bottom, Journal of Applied Thermal Engineering 27 (2007) 1036-1042.

[2] K.M. Khanafer, A.M. Al-Amiri, I. Pop, Numerical simulation of unsteady mixed convection in a driven cavity, using an externally excited sliding lid, European Journal of Mechanics- B/Fluids 26 (2007) 669-687.

[3] S. M. Aminossadati, B. Ghasemi, A numerical study of mixed convection in a horizontal channel with a discreet heat source in an open cavity, European Journal of Mechanics- B/Fluids 28 (2009) 590-598.

[4] K.Venkatasubbaiah, The effect of buoyancy on the stability mixed convection flow over a horizontal plate, European Journal of Mechanics - B/Fluids 30 (2011) 526-533.

[5] X.Q. Wang, A.S. Mujumdar, Heat transfer characteristics of nanofluids: a review, International Journal of Thermal Science 46 (2007) 1-19.

[6] J. Choi, Y. Zhang, Numerical simulation of laminar forced convection heat transfer of Al_2O_3-water nanofluid in a pipe with return bend, International Journal of Thermal Science 55 (2012) 90-102.

[7] W. Daungthongsuk, S.Wongwises,A critical review of convective heat transfer of nanofluids, Renewable & Sustainable Energy Reviews 11 (2007) 797-817.

[8] P.K. Namburu, D.K. Das, K.M. Tanguturi, R.S. Vajjha, Numerical study of turbulent flow and heat transfer characteristics of nanofluids considering variable properties, International Journal of Thermal Science 48 (2009) 290-302.

[9] R.K. Tiwari, M.K. Das, Heat transfer augmentation in a two-sided lid-driven differentially heated square cavity utilizing nanofluids, International Journal of Heat and Mass Transfer 50 (2007) 2002–2018.

[11] M. Muthtamilselvan, P. Kandaswamy, J. Lee, Heat transfer enhancement of copper_water nanofluids in a lid-driven enclosure, Communications in Nonlinear Science and Numerical Simulation 15 **(6)** (2009) 1501-1510.

[12] M. Shahi, A.H. Mahmoudi, F. Talebi, Numerical study of mixed convective cooling in a square cavity ventilated and partially heated from the below utilizing nanofluid, International Communications in Heat and Mass Transfer 37 (2010) 201–213.

[13] E. Abu-nada, A. J. Chamkha, Mixed convection flow in a lid-driven inclined enclosure filled with a nanofluid, European Journal of Mechanics - B/Fluids 29 (2010) 472-482.

[14] M. M. Billah, M. M. Rahman, M. Shahabuddin, A. K. Azad, Heat transfer enhancement of Copper-water nanofluids in an inclined lid-driven triangular enclosure, Journal of Scientific Research 3 **(2)** (2011) 525-538.

[15] A. J. Chamkha, E. Abu-nada, Mixed convection flow in single- and double-lid driven square cavities filled with water-Al2O3 nanofluid: Effect of viscosity models, European Journal of Mechanics - B/Fluids 36 (2012) 82-96.

[16] H. Khorasanizadeh, M. Nikfar, J. Amani, Entropy generation of Cu-water nanofluid mixed convection in a cavity, European Journal of Mechanics - B/Fluids 37 (2013) 143-152.

[17] G. A. Sheikhzadeh, H. Teimouri, M. Mahmoodi, Numerical study of mixed convection of nanofluid in a concentric annulus with rotating inner cylinder, Transport Phenomena in Nano and Micro Scales 1 (2013) 26-36.

[19] X. Wang, X. Xu, S.U.S. Choi, Thermal conductivity of nanoparticle–fluid mixture, Journal of Thermophysics and Heat Transfer 13 (1999) 474–480.

[20] P.K. Namburu, D.P. Kulkarni, D. Misra, D.K. Das, Viscosity of copper oxide nanoparticles dispersed in ethylene glycol and water mixture, Experimental Thermal and Fluid Science 32 (2007) 397-402.

[21] P.K. Namburu, D.P. Kulkarni, A. Dandekar, D.K. Das, Experimental investigation of viscosity and specific heat of silicon dioxide nanofluids, Micro Nano Letters 2 (2007) 67-71.

[22] B.C. Sahoo, R.S. Vajjha, R. Ganguli, G.A. Chukwu, D.K. Das, Determination of rheological behavior of aluminum oxide nanofluid and development of new viscosity correlations, Petroleum Science and Technology 27 (2009) 1757-1770.

[23] R.S. Vajjha, D.K. Das, Experimental determination of thermal conductivity of three nanofluids and development of new correlations, International Journal of Heat and Mass Transfer 52 (2009) 4675-4682.

[24] R.S. Vajjha, D.K. Das, Specific heat measurement of three nanofluids and development of new correlations, International Journal of Heat and Mass Transfer 131 (2009) 1-7.

[25] R.S. Vajjha, D.K. Das, B.M. Mahagaonkar, Density measurement of different nanofluids and their comparison with theory, Petroleum Science and Technology 27 (2009) 612-624.

[26] E. Abu-Nada, A.J. Chamkha, Effect of nanofluid variable properties on natural convection in enclosures filled with a CuO-EG-Water nanofluid, International Journal of Thermal Science 49 (2010) 2339-2352.

[27] E. Abu-Nada, Z. Masoud, H.F. Oztop, A. Campo, Effect of nanofluid variable properties on natural convection in enclosures, International Journal of Thermal Science 49 (2010) 479-491.

[28] G.A. Sheikhzadeh, M. Ebrahim Qomi, N. Hajialigol, A. Fattahi, Numerical study of mixed convection flows in a lid-driven enclosure filled with nanofluid using variable properties, Results in Physics 2 (2012) 5-13.

[29] S. Mazrouei Sebdani, M. Mahmoodi, S. M. Hashemi, Effect of nanofluid variable properties on mixed convection in a square cavity, International Journal of Thermal Science 52 (2012) 112-126.

[30] C.H. Chon, K.D. Kihm, S.P. Lee, S.U.S. Choi Empirical correlation finding the role of temperature and particle size for nanofluid (Al_2O_3) thermal conductivity enhancement, Applied Physics Letters 87 (2005) 153107.

[31] B.C. Pak, Y.I. Cho, Hydrodynamic and heat transfer study of dispersed fluids with submicron metallic oxide particles, Experimental Heat Transfer 11 (1999) 151-170.

[32] ASHRAE Handbook, Fundamentals. American Society of Heating, Refrigerating and Air-Conditioning Engineers Inc., Atlanta, GA, 2005.

[33] F.P. Incropera, D.P. DeWitt, Introduction to Heat Transfer, third ed. John Wiley & Sons, Inc., New York, 1996.

[34] R.S. Vajjha, D.K. Das, D.P. Kulkarni, Development of new correlations for convective heat transfer and friction factor in turbulent regime for nanofluids, International Journal of Heat and Mass Transfer 53 (2010) 4607-4618.

[35] S.V. Patankar, Numerical Heat Transfer and Fluid Flow, McGraw-Hill, 1980.

[36] B. Ghasemi, S. M. Aminossadati, Natural convection heat transfer in an inclined enclosure filled with a Water-Cuo Nanofluid, Numerical Heat Transfer 55 (2009) 807-823.